Available online at www.sciencedirect.com
SCIENCE DIRECT®
Biochemical Pharmacology 66 (2003) 511–517
Biochemical Pharmacology
www.elsevier.com/locate/biochempharm

DNA damage and expression of checkpoint genes *p21*$^{WAF1/CIP1}$ and *14-3-3* σ in taurine-deficient cardiomyocytes

Olga Golubnitschaja[a,*], Heike Moenkemann[a], Kerstin Kim[a], Mahmood S. Mozaffari[b]

[a]*Department of Radiology, Division of Molecular/Experimental Radiology, University of Bonn, Sigmund-Freud-Str. 25, D-53105 Bonn, Germany*
[b]*Department of Oral Biology and Maxillofacial Pathology, Medical College of Georgia, Augusta, GA 30912-1128, USA*

Received 13 November 2002; accepted 1 April 2003

Abstract

Objective: Taurine depletion is associated with development of cardiomyopathy. Further, oxidative stress is advanced as a critical factor mediating the effect of taurine deficiency on target organs. However, the molecular mechanism(s) linking taurine deficiency with the development of cardiomyopathy remains elusive. Since transition between apoptotic degeneration and cell proliferation in stress conditions is regulated at cell cycle checkpoints, we determined the expression of two such genes, namely *p21*$^{WAF1/CIP1}$ and *14-3-3* σ as well as *p53* that are responsible for oxidative stress and DNA damage. We also carried out quantitative determination of DNA damage. *Methods*: Cardiomyocytes from β-alanine-induced taurine-depleted (TD) rats were used for this investigation. Single- and double-stranded DNA damage was quantified using comet assay analysis. Western blot and two-dimensional polyacrylamide gel electrophoresis with immunoblotting analysis were applied for protein analysis. *Results*: Comet assay analysis indicated that the extent of double-stranded DNA damage was greater in TD than in control cardiomyocytes. Whereas only traces of both *p53* and *p21*$^{WAF1/CIP1}$ and no detectable expression of *14-3-3* σ were found in cardiomyocytes of control animals, the TD cardiomyocytes expressed all three genes. *Conclusions*: DNA damage and the consequent up-regulation of checkpoint proteins observed in TD cardiomyocytes indicate the involvement of cell cycle control mechanisms in the effect of taurine deficiency on cardiomyocytes. Single- and double-stranded DNA damage and the consequent arrest of cell proliferation in both G_1 and G_2 phases of the cell cycle induced by checkpoint proteins may trigger the cardiomyopathy that is associated with taurine deficiency.

Keywords: Taurine depletion; Cardiomyocytes *ex vivo*; DNA damage; Comet assay; Checkpoint proteins; Gene expression

1. Introduction

Taurine is a conditionally essential amino acid. It is not incorporated into proteins but is found in the free form in many tissues. In the heart it is found in high concentrations accounting for about 50% of the free amino acid pool [1]. The exact role of taurine in the heart remains elusive although a number of actions have been attributed to it. Among its putative effects are modulation of ion transport mechanisms and alterations in membrane structure and function [2,3]. These actions of taurine are apparently of consequence for the myocardium since both drug- and nutritionally-induced TD result in the development of cardiomyopathy that is manifested as impairment in both diastolic and systolic functions [3–6]. By contrast, taurine supplementation reverses cardiomyopathy in TD animals and also confers beneficial effects in patients with heart failure [3–5,7].

While the impact of TD on myocardial energy metabolism and contractile function have been the focus of many investigations [3–7], less is known regarding the impact of taurine deficiency on the potential triggering mechanism(s) of cardiomyopathy. Oxidative stress is proposed to be the pathogenic mechanism linking TD to the ultimate manifestation of cardiomyopathy. This contention is supported by several lines of evidence. First, taurine deficiency is associated with heart failure in animals and human subjects [3–6]. Second, taurine deficiency is associated

* Corresponding author. Tel.: +49-228-287-5982; fax: +49-228-287-4457.
E-mail address: Olga.Golubnitschaja@ukb.uni-bonn.de (O. Golubnitschaja).
Abbreviations: TD, taurine depletion; dsDNA, double-stranded DNA; ssDNA, single-stranded DNA.

0006-2952/$ – see front matter
doi:10.1016/S0006-2952(03)00285-5

with oxidative stress [4]. Third, the protective effects of taurine on target organs are attributed, in part, to its antioxidant property [4,8,9].

It is noteworthy, however, that taurine cannot directly scavenge reactive oxygen species and thus needs to function indirectly to reduce oxidative stress. Cellular response to oxidative stress is generally controlled at cell cycle checkpoints. Cell proliferation and progression into the DNA synthesis phase of the cell cycle are inhibited by the interaction of the P53-inducible $p21^{WAF1/CIP1}$ gene with the cdk2/cyclin E complex [10–13]. There is an excellent correlation between *p53* gene expression, capability for G_1 arrest, and $p21^{WAF1/CIP1}$ induction after oxidative DNA damage [14,15]. On the other hand, the arrest of the cell cycle in the G_2 phase is controlled by 14-3-3 σ. The expression of this gene also prevents apoptosis [16]. Apparently, 14-3-3 σ sequesters the mitotic initiation complex, cdc2/cyclin B1, in the cytoplasm after DNA damage. This prevents cdc2/cyclin B1 from entering the nucleus where the protein complex would normally initiate mitosis. In this manner, 14-3-3 σ induces G_2 arrest and allows the repair of damaged DNA [17,18].

The ability of both $P21^{WAF1/CIP1}$ and 14-3-3 σ to keep intracellular control over the DNA quality under stress conditions directs the regulation cascade in the transition between proliferation and apoptotic degeneration. In the heart there is a balance between the stimuli that induce cell growth (e.g. hypertrophy and hyperplasia) and those that induce programmed cell death [19,20]. Further, there are similarities and overlap among the mechanisms that regulate apoptosis and cell growth [21–23]. Therefore, cell cycle control may be the key event in the regulation of the cell population in the myocardium. It is likely that taurine exerts its antioxidant effect, at least in part, through modulation of the molecular events at the level of cell cycle checkpoints. By contrast, one would expect that taurine deficiency would cause oxidative stress resulting in DNA damage thereby affecting key events in the cell cycle. Since taurine deficiency results in myocardial dysfunction [3–6], we carried out an *ex vivo* investigation of the expression of these two stress responsible genes combined with quantitative determination of dsDNA damage which exerts the most toxic effects on genes.

2. Materials and methods

2.1. Experimental taurine depletion (TD)

Seven-week-old male Sprague–Dawley rats were obtained from Harlan Laboratories. All rats were maintained 2 per cage at constant humidity (60 ± 5%), temperature (24 ± 1°), and light cycle (06:00–18:00 hr). Two days after arrival, the animals were randomly assigned to two groups: one group received drinking water containing 3% β-alanine (TD group; N = 6) and the control group (N = 6) received only tap water. β-Alanine inhibits cellular uptake of taurine and its administration in the drinking water significantly reduces tissue taurine content (∼40%) [24,25]. It is noteworthy that several lines of evidence indicate that the manifested alterations in the TD rat relates to taurine deficiency than the taurine depleting agent [24,25]. Food and drinking fluid were available *ad lib.* throughout the study. Three weeks after initiation of the TD regimen, the animals were decapitated and the heart removed from each animal and immediately placed in liquid nitrogen. The hearts were kept at −80° until assayed.

2.2. Laser microdissection (LMD)

The frozen heart samples from both TD and control rats were used for LMD sections of cardiomyocytes with the ''Microbeam-MOMeNT'' technique as described earlier [26]. Serial sections of 5 μm thickness were cut, placed on numbered Superfrost/Plus slides (Fisher) and immediately placed on dry ice. The numbered sections were air dried, fixed in 70% EtOH and washed with sterile water. A Laser-Pressure-Catapulting device was used to collect specimen focusing onto the collection substrate using 40× magnifying objective. The laser cut tissue spots with cardiomyocytes were collected in sterile tubes, and stored at −80° until analysis.

2.3. Western blot analysis

Rat cardiomyocytes were lysed by homogenization in lysis buffer [9 M urea (Merck); 1% DTT (Sigma); 2% CHAPS (Merck); 0.8% Bio-Lyte pH 3–10 (Bio-Rad); 5 mM Pefabloc (Roche)] followed by centrifugation. The protein concentration in the supernatant was quantified by the DC-Protein Assay (Cat. No. 161-0318, Bio-Rad). Fourty μg protein of each sample were loaded onto 12% SDS–polyacrylamide gels and electrophoresed to resolve proteins. The proteins were then transferred to nitrocellulose membranes (Schleicher and Schuell). Thereafter, they were incubated in blocking buffer (58 mM $NaHPO_4$, 17 mM NaH_2PO_4, 68 mM NaCl, 5% non-fat dry milk powder; 0.1% Tween 20) for 1 hr at room temperature. Incubation with primary antibody was performed using a 1:250 dilution of either anti-human-14-3-3 σ or anti-human-$P21^{WAF1/CIP1}$ for 1 hr at room temperature in washing buffer I (58 mM $NaHPO_4$, 17 mM NaH_2PO_4, 68 mM NaCl, 1% non-fat dry milk powder, 0.1% Tween 20); these antibodies display cross-reactivity with the rat proteins. The membranes were then washed four times in the same solution. The horseradish peroxidase-labeled anti-goat secondary antibody was incubated with the membranes for 1 hr at room temperature in washing buffer I. This was followed by three washes in washing buffer II (58 mM $NaHPO_4$, 17 mM NaH_2PO_4, 68 mM NaCl, 1% non-fat dry milk powder; 0.3% Tween 20) and three washes in washing buffer I. Then the membranes were reacted with

chemiluminescent reagent ECL plus (Cat. No. RPN 2132, Amersham Pharmacia) and processed for autoradiography.

2.4. Two-dimensional PAGE (2D-PAGE) and immunoblotting analysis

A 400 μg aliquot of each protein sample was used for 2D-PAGE separation followed by immunoblotting analysis. One-dimensional separation was performed in immobilized pH gradient gels (IPG-Strips, Bio-Rad) through the electric isofocusing of proteins in the range of pH 4–7 as described by the supplier. 125 μL protein samples containing rehydration buffer (8 M urea, 10 mM DTT, 1% CHAPS, 0.25% Bio-Lyte, pH 4–7) were loaded on the IPG-Strips and subjected to 14 kVhr overnight at 20° in a PROTEAN IEF Cell. After this one-dimensional protein separation the extruded IPG-Strips were equilibrated in gel equilibration buffer I (50 mM Tris–HCl, 6 M urea, 30% glycerol, 2% SDS, 1% DTT). This was followed by equilibration in buffer II (50 mM Tris–HCl, 6 M urea, 30% glycerol, 2% SDS and 260 mM iodacetamide) for 10 min before loading them onto polyacrylamide gels (12% SDS–PAGE) for the two-dimensional resolution in Mini-PROTEAN 3 (Bio-Rad). For the determination of sizes of the separated proteins a colored protein standard (Cat. No. 161-0318, Bio-Rad) was loaded onto the gels. After electrophoresis the separated proteins were electrotransferred to nitrocellulose membranes and immunoblotted as described in Western blot analysis for the 14-3-3 σ protein detection.

2.5. Comet assay analysis

2.5.1. Principle

dsDNA and ssDNA damage was measured as increased migration of DNA using the single-cell gel electrophoresis technique (comet assay). The assays were conducted under neutral and alkaline conditions to detect dsDNA and ssDNA breaks, respectively. The measurement was performed in isolated cardiomyocytes *ex vivo*. The comet assay (Trevigen, Inc., Cat. No. 4250-050-K) provides a simple and effective method for evaluating DNA damage in cells. The principle of the assay is based upon the ability of cleaved DNA fragments to migrate out of the nucleus under the influence of an electric field. Intact DNA molecules migrate slower and remain within the confines of the nucleoid when a current is applied. Evaluation of the DNA ''comet'' tail shape and migration pattern allows for assessment of DNA damage. This method has been described in detail previously [27–31].

2.5.2. Experimental

Isolated cardiomyocytes were calculated in each sample and immobilized in a bed of low melting point agarose with a cell density of about 200–300 cells per sample. Following gentle cell lysis and electrophoretic separation of fragmented DNA, the slides were stained with SYBR® Green, a DNA intercalating fluorescence dye. DNA fragmentation was evaluated using the imaging system from Olympus, Germany.

2.5.3. Microscope slide analysis

The comets were visualized under a fluorescent microscope (Olympus) at 40×, with a 515–560 nm exciting filter and a 590 nm barrier filter, and analyzed by image analysis (SIS). At least 100 comets were analyzed for each data point.

2.5.4. Comet measurement

Damage was assigned to four classes based on the visual aspect of the comets, considering the extent of DNA migration [30,32]. Comets with a bright head and almost no tail were classified as class 1 with minimal DNA damage. Comets with no visible head and a long diffuse tail were classified as class 4 (severely damaged/apoptotic cells). Comets with intermediate characteristics were assigned to classes 2 and 3 dependent on the ratio $R = T/r$, where T is a length of comet's tail and r is a radius of comet's head. The characteristic value of R for class 1 is 1 ($T \approx r$) and for class 4 is ∞ ($r = 0$). Comets with values $1 < R < 3$ were classified as class 2 (see Section 3).

2.5.5. DNA damage evaluation

DNA damage (DD) and a relative DNA damage (RDD) were calculated using Eqs. (1) and (2) described in literature [33,34] and modified for four classes observed in our case:

$$\mathrm{DD} = \frac{n_2 + 2\,n_3 + 3\,n_4}{\Sigma/100} \tag{1}$$

$$\mathrm{RDD} = \left(\frac{\mathrm{DD}}{\mathrm{DD}_0}\right) \times 100\% \tag{2}$$

where DD is the DNA damage, n_2–n_4 are the amount of calculated comets in classes 2, 3 and 4, respectively, Σ is the total number of scored comets, including class 1 with no DNA damage, RDD is the relative DNA damage calculated for the cardiomyocytes of TD rats, and DD_0 is the DD in samples from the control group.

2.5.6. Statistical analysis

All statistical analyses were done using the SPSS software (version 8.0). Statistical significance was calculated by the two-sided unpaired Student's *t*-test.

3. Results

3.1. Comet assay analysis

Fig. 1 shows a representative example of each of the four classes of comets. Comets with a bright head and almost no tail were classified as class 1 indicating minimal DNA

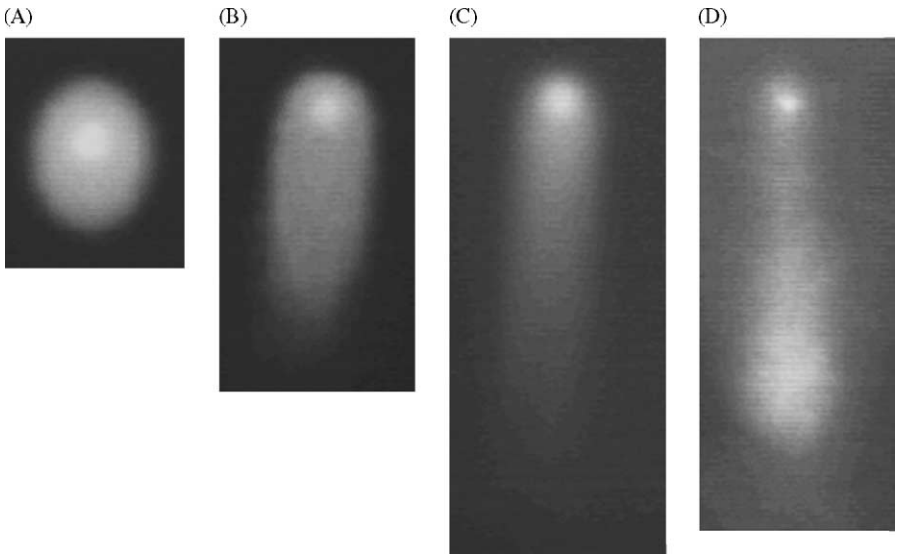

Fig. 1. Comet classification. (A) Comets with a bright head and almost no tail were classified as class 1 with minimal DNA damage. (D) Comets with no visible head and a long diffuse tail were classified as class 4 (completely fragmented DNA). Comets with intermediate characteristics were assigned to classes 2 (B) and 3 (C).

damage (Fig. 1A). By contrast, comets with no visible head and a long diffuse tail were classified as class 4 indicating complete fragmentation of DNA (Fig. 1D). Comets with intermediate characteristics were assigned to classes 2 and 3 (Fig. 1B and C). Figs. 2 and 3 show significant increase in both (A) dsDNA and (B) ssDNA damage in cardiomyocytes of TD compared to the control rats.

(A) *dsDNA breaks*: The ratio of the most damaged (class 4) to the intact dsDNA (class 1) molecules is about 3 for the control and about 14 for the TD group (Fig. 2). Cardiomyocytes of the control rats displayed damaged dsDNA molecules belonging to classes 2, 3 and 4 that are, collectively, nearly 6-fold higher than the amount of comets belonging to class 1. By contrast, the TD cardiomyocytes displayed nearly 19 times as much damaged dsDNA than intact DNA molecules. The relationship of classes 2 and 3 comets were similar between the two groups (Fig. 2). The calculated mean value of relative DNA damage in cardiomyocytes of TD rats under neutral conditions is $128 \pm 6\%$.

(B) *ssDNA breaks*: The difference between the ratios for class 4 to class 1 for the control and TD groups is considerably greater under alkaline than under neutral conditions; the values are about 7 and 60 for the control and TD group, respectively (Fig. 3). The ratio of the completely damaged ssDNA to intact DNA molecules was about 13 for the control group, whereas it was about 66 for the TD group. Similar to the results under neutral conditions there was no significant difference in the relationship of class 2 and class 3 between the two groups. The calculated mean value of relative DNA damage in cardiomyocytes of TD rats under alkaline conditions is $128 \pm 9\%$ which is similar to that observed under neutral conditions ($128 \pm 6\%$).

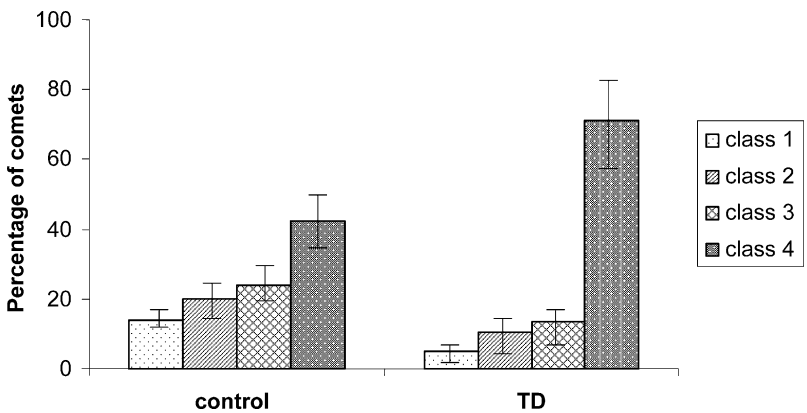

Fig. 2. Results of comparative comet assay analysis under neutral conditions with calculated standard deviations in cardiomyocytes of TD (A) and control (B) rats. Data are means ± SD.

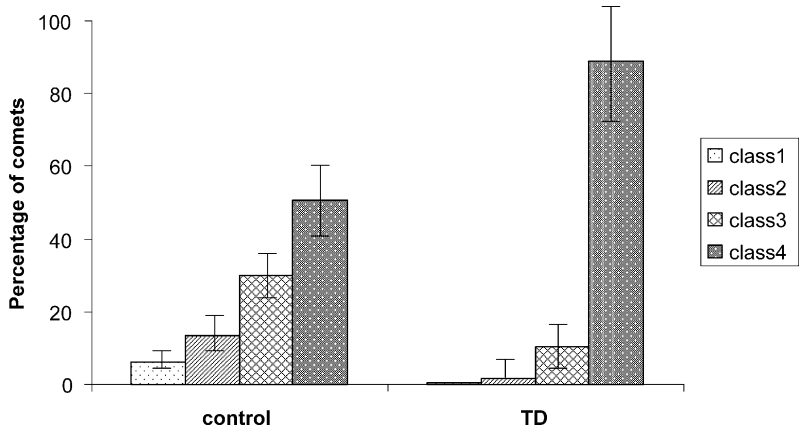

Fig. 3. Results of comparative comet assay analysis under alkaline conditions with calculated standard deviations in cardiomyocytes of TD (A) and control (B) rats. Data are means ± SD.

3.2. Western blot analysis

Western blot analysis shows an enhanced gene expression of both *p21*$^{WAF1/CIP1}$ and *p53* in cardiomyocytes of TD rats but only traces of both proteins were detected in the control group (Figs. 4 and 5). There were no significant quantitative differences in the gene expression rate of both *p21*$^{WAF1/CIP1}$ and *p53* among individual samples within the group of TD rats (data not shown).

3.3. Two-dimensional immunoblots (TDIBs)

Western blot experiments indicated that the absolute gene expression rate of *14-3-3 σ* is relatively weak (data are not shown). Therefore, the more sensitive technique of 2D-PAGE followed by immunoblotting (two-dimensional immunoblots; TDIBs) was used for expression analysis of *14-3-3 σ*. The cardiomyocytes of the TD rats displayed a single spot of about 31 kDa on TDIBs that corresponds to the 14-3-3 σ protein (Fig. 6A); its isoelectric point was determined to be 6.8. However, no detectable expression of *14-3-3 σ* was noted in the control group (Fig. 6B).

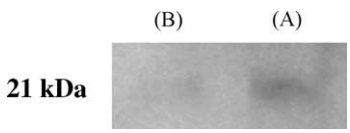

Fig. 4. Western blot analysis of *p21*$^{WAF1/CIP1}$ gene expression in cardiomyocytes of TD (lane A) and control (lane B) rats.

Fig. 5. Western blot analysis of *p53* gene expression in cardiomyocytes of TD (lane A) and control (lane B) rats.

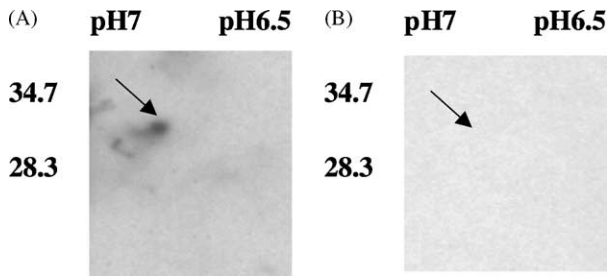

Fig. 6. Two-dimensional immunoblots (TDIBs) analysis of *14-3-3 σ* gene expression in cardiomyocytes. While, no spots were observed in TDIBs of the control group (B), a single spot was detected (arrow) in TDIBs of TD group (A).

4. Discussion

This study shows that TD promotes DNA damage and causes activation of events that are involved in cell cycle arrest. This contention is supported by the observation that whereas no detectable gene expression of 14-3-3 σ and only traces of P53 and P21$^{WAF1/CIP1}$ were found in cardiomyocytes of the control group, all three genes were induced in cardiomyocytes of TD rats. Taken together, these findings suggest that arrest of cardiomyocyte growth is triggered in both G_1 and G_2 phases of the cell cycle, an effect due to the accompanying DNA damage in TD cardiomyocytes. These molecular events could potentially cause degeneration of cardiomyocytes, and thereby trigger the development of cardiomyopathy under taurine deficiency conditions [5,35].

Increasing evidence suggests that dietary taurine supplementation confers protective effects on target organs including the heart. Several mechanisms have already been proposed to account for the beneficial effect of taurine in heart failure. First, taurine is an important osmoregulator and exerts multiple effects on ion transport mechansims [2,3,36]. Further, recent evidence indicates that taurine's osmoregulatory function is associated with a modification of the osmolarity sensor protein ENVZ expression in the heart [37]. Second, taurine modulates kidney function by promoting natriuresis and diuresis, thereby affecting body

fluid homeostasis [24]. These actions of taurine could be of potential benefit in heart failure, a condition associated with fluid and sodium retention. Third, taurine mediates a modest positive ionotropic effect by regulating $[Ca^{2+}]_i$, $[Na^+]_i$ and Na^+/Ca^{2+} exchanger activity [3,7,38]. Fourth, taurine opposes some of the actions of angiotensin II including those on Ca^{2+} transport, protein synthesis and angiotensin II signaling [38,39]. The net effect would be attenuation of angiotensin II-mediated events such as induction of cardiac hypertrophy, myocardial remodeling and volume overload [38].

Despite recognition of the diverse mechanisms by which taurine therapy exerts its multiple effects, the molecular basis for the beneficial effect of taurine treatment in heart failure has not received adequate attention. In order to get an insight into the effect of taurine on molecular events regulating the cell cycle, we used the TD rat model that has been shown to develop a number of abnormalities in both myocardial function and bioenergetics [3,40,41]. Since taurine is an important intracellular antioxidant, its deficiency is believed to augment cellular oxidative damage [4]. However, the consequences of taurine deficiency-induced oxidative stress on the regulatory mechanisms that determine the balance between proliferation and degenerative reduction of cardiomyocytes are not clear.

Cell growth and degeneration are ultimately controlled by cell cycle regulatory checkpoint proteins. Progression of the cell cycle events requires that cyclin-dependent kinases become activated. Cyclin kinase inhibitors inactivate cyclin-dependent kinases, causing cell cycle arrest [42]. The expression rate of both genes $p21^{WAF1/CIP1}$ and *14-3-3 σ* is elevated by DNA damage in order to trigger cell cycle arrest and DNA repair [10,17,43]. The results of the comet assay under both neutral and alkaline conditions clearly indicate that TD is accompanied by significant DNA damage in cardiomyocytes thereby facilitating the expression of the *p53*, $p21^{WAF1/CIP1}$ and *14-3-3 σ* genes. It is noteworthy, however, that the relatively high dsDNA fragmentation of control cardiomyocytes is in agreement with high rates of cell death reported by other investigators in normal adult human hearts and those of mice and rats [19]. Nonetheless, our observations suggest that in cardiomyocytes taurine exerts a regulatory/modulatory role on cell cycle control. The effects of taurine on these aspects may represent an essential component against cardiac tissue degeneration. These beneficial effects would be lacking in TD cardiomycytes thereby promoting degenerative changes. This may explain the beneficial effects of taurine therapy in reversal of TD cardiomyopathy [5]. This contention is supported by the emerging evidence indicating that taurine supplementation protects pancreatic β-cell degeneration in a dose-dependent manner in streptozotocin-induced diabetic rats [44]. Therefore, it is likely that DNA molecules are the primary target, the damage to which results in a non-physiological depletion of NAD *via* activation of poly(ADP-ribose) synthetase (PARP). PARP is an abundant nuclear protein functioning as a DNA nick-sensor enzyme. Upon binding to DNA breaks, activated PARP cleaves NAD(+) into nicotinamide and ADP-ribose and polymerizes the latter onto nuclear acceptor proteins including histones, transcription factors, and PARP itself. Poly-ADP-ribosylation contributes to DNA repair and to the maintenance of genomic stability. On the other hand, oxidative stress-induced overactivation of PARP consumes NAD(+) and consequently ATP, culminating in cell dysfunction or necrosis. This cellular suicide mechanism has been implicated in the pathomechanism of stroke, myocardial ischemia, diabetes, diabetes-associated cardiovascular dysfunction, shock, etc. [45]. Inhibition of the poly(ADP-ribose) synthetase results in multiple effects including an increase in the survival rate of pancreatic β-cells, without preventing DNA strand breaks, and considerably increases the frequency of islet β-cell tumors [46]. In this regard, it is noteworthy that the ability of different cell types to resist the effect of reactive oxygen species may ultimately lead to the identification of biomarkers of cellular resistance in pathological conditions (e.g. diabetes mellitus) [47–49].

In conclusion, TD causes DNA damage accompanied by the up-regulation of key genes that regulate the cell cycle machinery, namely *p53*, $p21^{WAF1/CIP1}$ and *14-3-3 σ* in cardiomyocytes. Since TD is associated with the development of cardiomyopathy, the relevance of these molecular events to the ultimate manifestation of cardiomyopathy caused by TD represents a fertile area for further investigation.

Acknowledgments

This study was supported by Bio-Rad, USA (OG) and Taisho Pharmaceutical company of Japan (MSM).

References

[1] Huxtable RJ. The physiological actions of taurine. Physiol Rev 1992;72:101–63.
[2] Labudova O, Yeghiazarjan C, Hoger H, Lubec G. Taurine modulates expression of transporters in rat brain and heart. Amino Acids 1999;17:301–13.
[3] Schaffer S, Solodushko V, Azuma J. Taurine-deficient cardiomyopathy: role of phospholipids, calcium and osmotic stress. In: Della Corte L, Huxtable RJ, Sgaragli G, Tipton KF, editors. Taurine 4: taurine and excitable tissues. New York: Kluwer Academic Publishers; 2000. p. 57–69.
[4] Sole MJ, Jeejeebhoy KN. Conditioned nutritional requirements: therapeutic relevance to heart failure. Herz 2002;27:174–8.
[5] Pion PD, Kittleson MD, Rogers QR, Morris JG. Myocardial failure in cats associated with low plasma taurine: a reversible cardiomyopathy. Science 1987;237:764–8.
[6] Novotny MJ, Hogan PM, Paley DM, Adams HR. Systolic and diastolic dysfunction of the left ventricle induced by taurine deficiency in cats. Am J Physiol 1991;261:H121–7.
[7] Azuma J, Sawamura A, Awata N. Usefulness of taurine in chronic congestive heart failure and its prospective application. Jpn Circ J 1992;56:95–9.

[8] Obrosova IG, Fathallah L, Stevens MJ. Taurine counteracts oxidative stress and nerve growth factor deficit in early experimental diabetic neuropathy. Exp Neurol 2001;172:211–9.
[9] Kondo Y, Toda Y, Kitajima H, Oda H, Nagate T, Kameo K, Murakami S. Taurine inhibits development of atherosclerotic lesions in apolipoprotein E-deficient mice. Clin Exp Pharmacol Physiol 2001;28:809–15.
[10] Gartel AL, Serfas MS, Tyner AL. p21-negative regulator of the cell cycle. Proc Soc Exp Biol Med 1996;213:138–49.
[11] Mantel C, Braun SE, Reid S, Henegariu O, Liu L, Hangoc G, Broxmeyer HE. p21(cip-1/waf-1) deficiency causes deformed nuclear architecture, centriole overduplication, polyploidy, and relaxed microtubule damage checkpoints in human hematopoietic cells. Blood 1999;93:1390–8.
[12] Chen J, Saha P, Kornbluth S, Dynlacht BD, Dutta A. Cyclin-binding motifs are essential for the function of p21CIP1. Mol Cell Biol 1996;16:4673–82.
[13] Ogryzko VV, Wong P, Howard BH. WAF1 retards S-phase progression primarily by inhibition of cyclin-dependent kinases. Mol Cell Biol 1997;17:4877–82.
[14] Coffman FD, Studzinski GP. Differentiation-related mechanisms which suppress DNA replication. Exp Cell Res 1999;248:58–73.
[15] Stein GH, Drullinger LF, Soulard A, Dulic V. Differential roles for cyclin-dependent kinase inhibitors p21 and p16 in the mechanisms of senescence and differentiation in human fibroblasts. Mol Cell Biol 1999;19:2109–17.
[16] Samuel T, Weber HO, Rauch P, Verdoodt B, Eppel JT, McShea A, Herineking H, Funk J. The G_2/M regulator 14-3-3 σ prevents apoptosis through sequestration of Bax. J Biol Chem 2001;276:45201–6.
[17] Hermeking H, Lengauer C, Polyak K, He TC, Zhang L, Thiagalingam S, Kinzler KW, Vogelstein B. 14-3-3 sigma is a *p53*-regulated inhibitor of G_2/M progression. Mol Cell 1997;1:3–11.
[18] Chan TA, Hermeking H, Lengauer C, Kinzier KW, Vogelstein B. 14-3-3 sigma is required to prevent mitotic catastrophe after DNA damage. Nature 1999;401:535–7.
[19] Nadal-Ginard B. Generation of new cardiomyocytes in the adult heart: prospects of myocardial regeneration as an alternative to cardiac transplantation. Rev Esp Cardiol 2001;54:543–50.
[20] Kang YJ. Molecular and cellular mechanisms of cardiotoxicity. Environ Health Perspect 2001;109:27–34.
[21] von Harsdorf R, Li PF, Dietz R. Signaling pathways in reactive oxygen species-induced cardiomyocyte apoptosis. Circulation 1999;99:2934–41.
[22] Ikeda S, Hamada M, Hiwada K. Contribution of non-cardiomyocyte apoptosis to cardiac remodeling that occurs in the transition from compensated hypertrophy to heart failure in spontaneously hypertensive rats. Clin Sci (London) 1999;97:239–46.
[23] Yussman MG, Toyokawa T, Odley A, Lynch RA, Wu G, Colbert MC, Aronow BJ, Lorenz JN, Dorn II GW. Mitochondrial death protein Nix is induced in cardiac hypertrophy and triggers apoptotic cardiomyopathy. Nat Med 2002;8:725–30.
[24] Mozaffari MS, Schaffer D. Taurine modulates arginine vasopressin-mediated regulation of renal function. J Cardiovasc Pharmacol 2001;37:742–50.
[25] Allo SN, Bagby L, Schaffer SW. Taurine depletion, a novel mechanism for cardioprotection from regional ischemia. Am J Physiol 1997;273:H1956–61.
[26] Bohm M, Wieland I, Schutze K, Rubben H. Microbeam-MOMeNT: non-contact laser microdissection of membrane-mounted native tissue. Am J Pathol 1997;151:63–7.
[27] Ostling O, Johanson KJ. Microelectrophoretic study of radiation-induced DNA damages in individual mammalian cells. Biochem Biophys Res Commun 1984;123:291–8.
[28] Anderson D, Plewa MJ. The international comet assay workshop. Mutagenesis 1998;13:67–73.
[29] Malyapa RS, Bi C, Ahern EW, Roti Roti JL. Detection of DNA damage by the alkaline comet assay after exposure to low-dose gamma radiation. Radiat Res 1998;149:396–400.
[30] Lemay M, Wood KA. Detection of DNA damage and identification of UV-induced photoproducts using the comet assay kit. Biotechniques 1999;27:846–51.
[31] Wojewodzka M, Buraczewska I, Kruszewski M. A modified neutral comet assay: elimination of lysis at high temperature and validation of the assay with anti-single-stranded DNA antibody. Mutat Res 2002;518:9–20.
[32] Visvardis EE, Tassiou AM, Piperakis SM. Study of DNA damage induction and repair capacity of fresh and cryopreserved lymphocytes exposed to H_2O_2 and gamma-irradiation with the alkaline comet assay. Mutat Res 1997;383:71–80.
[33] Nascimento PA, da Silva MA, Oliveira EM, Suzuki MF, Okazaki K. Evaluation of radioinduced damage and repair capacity in blood lymphocytes of breast cancer patients. Braz J Med Biol Res 2001; 34:165–76.
[34] Jaloszynski P, Kujawski M, Czub-Swierczek M, Markowska J, Szyfter K. Bleomycin-induced DNA damage and its removal in lymphocytes of breast cancer patients studied by comet assay. Mutat Res 1997;385: 223–33.
[35] Pop-Busui R, Sullivan KA, Van Huysen C, Bayer L, Cao X, Towns R, Stevens MJ. Depletion of taurine in experimental diabetic neuropathy: implications for nerve metabolic, vascular, and functional deficits. Exp Neurol 2001;168:259–72.
[36] Suleiman MS. New concepts in the cardioprotective action of magnesium and taurine during the calcium paradox and ischaemia of the heart. Magnes Res 1994;7:295–312.
[37] Moenkemann H, Labudova O, Yeghiazarian K, Rink H, Hoeger H, Lubec G. Evidence that taurine modulates osmoregulation by modification of osmolarity sensor protein ENVZ-expression. Amino Acids 1999;17:347–55.
[38] Schaffer SW, Lombardini JB, Azuma J. Interaction between the actions of taurine and angiotensin II. Amino Acids 2000;18:305–18.
[39] Rao MR, Tao L. Effects of taurine on signal transduction steps induced during hypertrophy of rat heart myocytes. Adv Exp Med Biol 1998;442:137–43.
[40] Harada H, Allo S, Viyuoh N, Azuma J, Takahashi K, Schaffer SW. Regulation of calcium transport in drug-induced taurine-depleted hearts. Biochim Biophys Acta 1988;944:273–8.
[41] Lake N, Splawinski JB, Juneau C, Rouleau JL. Effects of taurine depletion on intrinsic contractility of rat ventricular papillary muscles. Can J Physiol Pharmacol 1990;68:800–6.
[42] Waga S, Hannon GJ, Beach D, Stillman B. The p21 inhibitor of cyclin-dependent kinases controls DNA replication by interaction with PCNA. Nature 1994;369:520–1.
[43] Li R, Waga S, Hannon GJ, Beach D, Stillman B. Differential effects by the p21 CDK inhibitor on PCNA-dependent DNA replication and repair. Nature 1994;371:534–7.
[44] Chang KJ. Effect of taurine and beta-alanine on morphological changes of pancreas in streptozotocin-induced rats. Adv Exp Med Biol 2000;483:571–7.
[45] Virag L, Szabo C. The therapeutic potential of poly(ADP-ribose) polymerase inhibitors. Pharmacol Rev 2002;54:375–429.
[46] Pieper AA, Brat DJ, Krug DK, Watkins CC, Gupta A, Blackshaw S, Verma A, Wang ZQ, Snyder SH. Poly(ADP-ribose) polymerase-deficient mice are protected from streptozotocin-induced diabetes. Proc Natl Acad Sci USA 1999;96:3059–64.
[47] Leinonen J, Lehtimaki T, Toyokuni S, Okada K, Tanaka T, Hiai H, Ochi H, Laippala P, Rantalaiho V, Wirta O, Pasternack A, Alho H. New biomarker evidence of oxidative DNA damage in patients with non-insulin-dependent diabetes mellitus. FEBS Lett 1997;417:150–2.
[48] Hinokio Y, Suzuki S, Hirai M, Chiba M, Hirai A, Toyota T. Oxidative DNA damage in diabetes mellitus: its association with diabetic complications. Diabetologia 1999;42:995–8.
[49] Mönkemann H, De Vriese AS, Blom HJ, Kluijtmans LA, Heil SG, Schild HH, Golubnitschaja O. Early molecular events in the development of the diabetic cardiomyopathy. Amino Acids 2002;23:331–6.